Available online at www.sciencedirect.com

SCIENCE DIRECT

Virology 336 (2005) 11–25

VIROLOGY

www.elsevier.com/locate/yviro

Progression from productive infection to integration and oncogenic transformation in human papillomavirus type 59-immortalized foreskin keratinocytes

Helena Spartz[a], Elizabeth Lehr[b], Benyue Zhang[a,c,d], Ann Roman[a,c,d], Darron R. Brown[a,b,*]

[a]*Department of Microbiology and Immunology, Indiana University School of Medicine, Indianapolis, IN 46202, USA*
[b]*Department of Medicine, Indiana University School of Medicine, Indianapolis, IN 46202, USA*
[c]*Walther Oncology Center, Indiana University School of Medicine, Indianapolis, IN 46202, USA*
[d]*Walther Cancer Institute, Indianapolis, IN 46202, USA*

Received 28 June 2004; returned to author for revision 8 October 2004; accepted 9 February 2005
Available online 12 April 2005

Abstract

Studies of changes in the virus and host cell upon progression from human papillomavirus (HPV) episomal infection to integration are critical to understanding HPV-related malignant transformation. However, there exist only a few in vitro models of both productive HPV infection and neoplastic progression on the same host background. We recently described a unique foreskin keratinocyte cell line (ERIN 59) that contains HPV 59 (a close relative of HPV 18). Early passages of ERIN 59 cells (passages 9–13) contained approximately 50 copies of episomes/cell, were feeder cell-dependent, and could be induced to differentiate and produce infectious virus in a simple culture system. We now report that late passage cells (passages greater than 50) were morphologically different from early passage cells, were feeder cell independent, and did not differentiate or produce virus. These late passage cells contained HPV in an integrated form. An integration-derived oncogene transcript was expressed in late passage cells. The E2 open reading frame was interrupted in this transcript at nucleotide 3351. Despite a lower viral genome copy number in late passage ERIN 59 cells, expression of E6/E7 oncogene transcripts was similar to early passage cells. We conclude that ERIN 59 cells are a valuable cell line representing a model of progression from HPV 59 episomal infection and virus production to HPV 59 integration and associated oncogenic transformation on the same host background.

Keywords: Human papillomavirus; Keratinocyte; ERIN 59

Introduction

Infection of the genital epithelium in both females and males with certain types of human papillomavirus (HPV) is associated with an increased risk of dysplasia and invasive malignancy (Koutsky, 1997; Schiffman and Brinton, 1995; Schiffman and Burk, 1997). These dysplastic lesions sometimes persist and progress to invasive cancers. In low-grade pre-neoplastic lesions the HPV genome generally exists in an episomal form, and the host cell can differentiate permitting production of infectious virus (Badaracco et al., 2002; Das et al., 1992; Evans et al., 2002; Gross and Pfister, 2004; Hernadi et al., 2004; Hopman et al., 2004; Hudelist et al., 2004; Lizard et al., 1998). Conversely, in high-grade lesions and cancers, the HPV genome usually is integrated into the host chromosomal DNA, the host cell differentiates aberrantly, and virus is not produced (Das et al., 1992; Hopman et al., 2004; Hudelist et al., 2004).

Several in vitro models developed from HPV immortalized keratinocytes have proven useful in studies of viral pathogenesis. Cell lines containing integrated viral sequences such as HeLa, CaSki, SiHa, and others were developed from cervical carcinomas and have proven valuable in studying the HPV-induced neoplastic phenotype (El Awady et al., 1987; Lazo, 1987; Stupar, 1989).

* Corresponding author. Department of Medicine, 545 Barnhill Drive, Indianapolis, IN 46202, USA. Fax: +1 317 274 1587.
E-mail address: darbrow@iupui.edu (D.R. Brown).

0042-6822/$ - see front matter © 2005 Elsevier Inc. All rights reserved.
doi:10.1016/j.virol.2005.02.026

In contrast, several cell lines derived from HPV-infected clinical specimens contain episomal HPV and have been valuable for studying other aspects of the viral life cycle. For example, CIN-612 cervical keratinocytes contain episomal HPV 31b (De Geest et al., 1993; Hummel et al., 1992; Ozbun, 2002; Ozbun and Meyers, 1997). The W12 cell line (also cervical keratinocytes) initially contained episomal HPV 16 in early passages but was found to have integrated HPV 16 sequences after in vitro passages (Alazawi et al., 2002; Flores and Lambert, 1997; Jeon et al., 1995; Stanley et al., 1989; Sterling et al., 1990) The CIN-612 and W12 cells require raft culturing systems for virus production. HPV 16 and HPV 31b have been maintained as episomes in these rafts, providing an additional method for analysis of the HPV life cycle. The UT-DEC-1 vaginal keratinocyte cell line contains episomal HPV 33 in early passage cells and integrated viral DNA in late passage cells (Auvinen et al., 1998; Hietanen et al., 1992; Peitsaro et al., 2002).

These cell lines have proven valuable for analyzing the differences in both virus and host between episomal and integrated viral forms. It is important to establish additional in vitro models to assess whether observations made in W12, CIN 612, and UT-DEC-1 are also seen for other high-risk HPV types, and in other genital keratinocytes of different genetic backgrounds.

We recently developed ERIN 59 cells, a foreskin keratinocyte cell line containing HPV 59, an oncogenic type related to HPV 18 and HPV 45 (Bryan et al., 2000; Lehr et al., 2003; Rho et al., 1994, 1996). Our prior studies indicated that ERIN 59 cells initially contained approximately 50 copies of

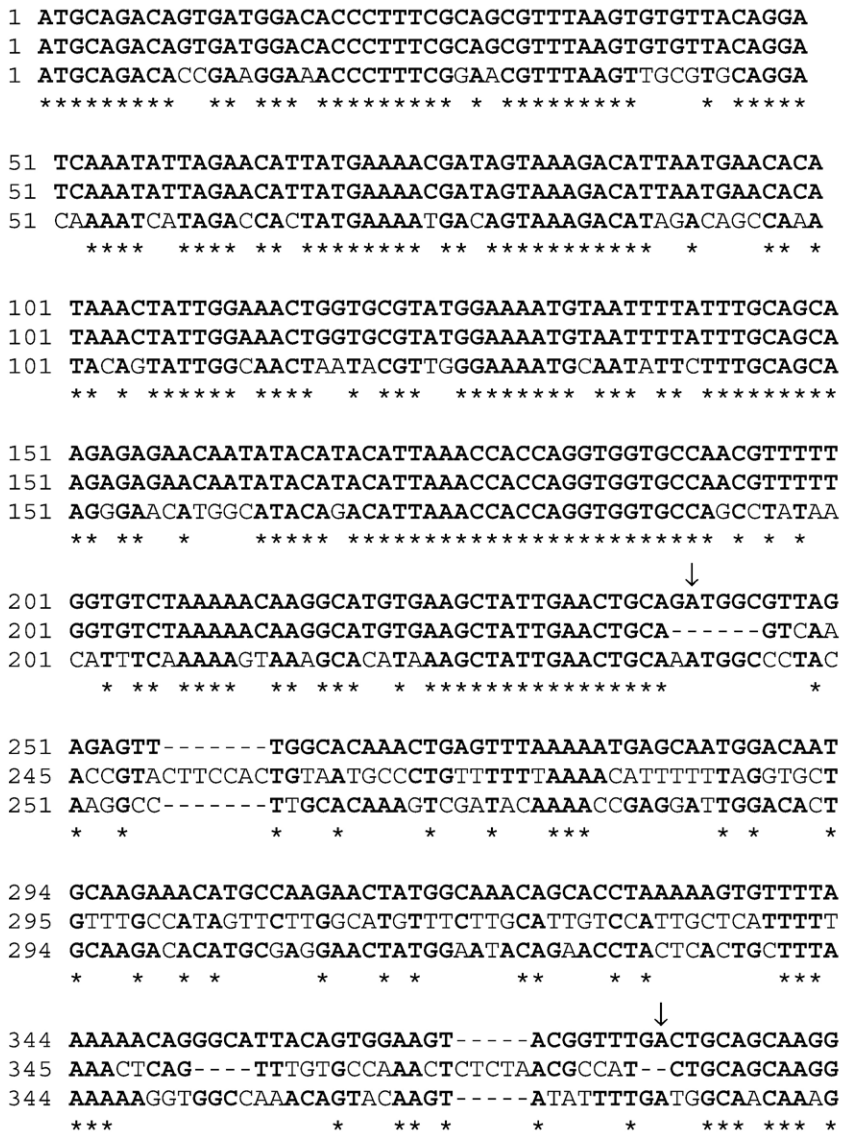

Fig. 1. Alignment of E2 DNA sequences from ERIN59 cells (top sequence), the published HPV 59 E2 DNA sequence (middle sequence), and the published HPV 18 E2 DNA sequence (bottom sequence). Nucleotides are indicated by single letter designation, and the number of the nucleotide within the E2 ORF is shown on the left side of the figure. Bold lettering indicates nucleotides matching with the sequence from ERIN59 cells. The star symbols (*) indicate matching nucleotides for all three sequences. The DNA sequence between E2 position 241, equivalent to HPV 59 position 2970 (arrow over the position), and E2 position 377, equivalent to HPV 59 position 3118 (arrow over the position), correspond to the putative inversion error in the published HPV 59 sequence.

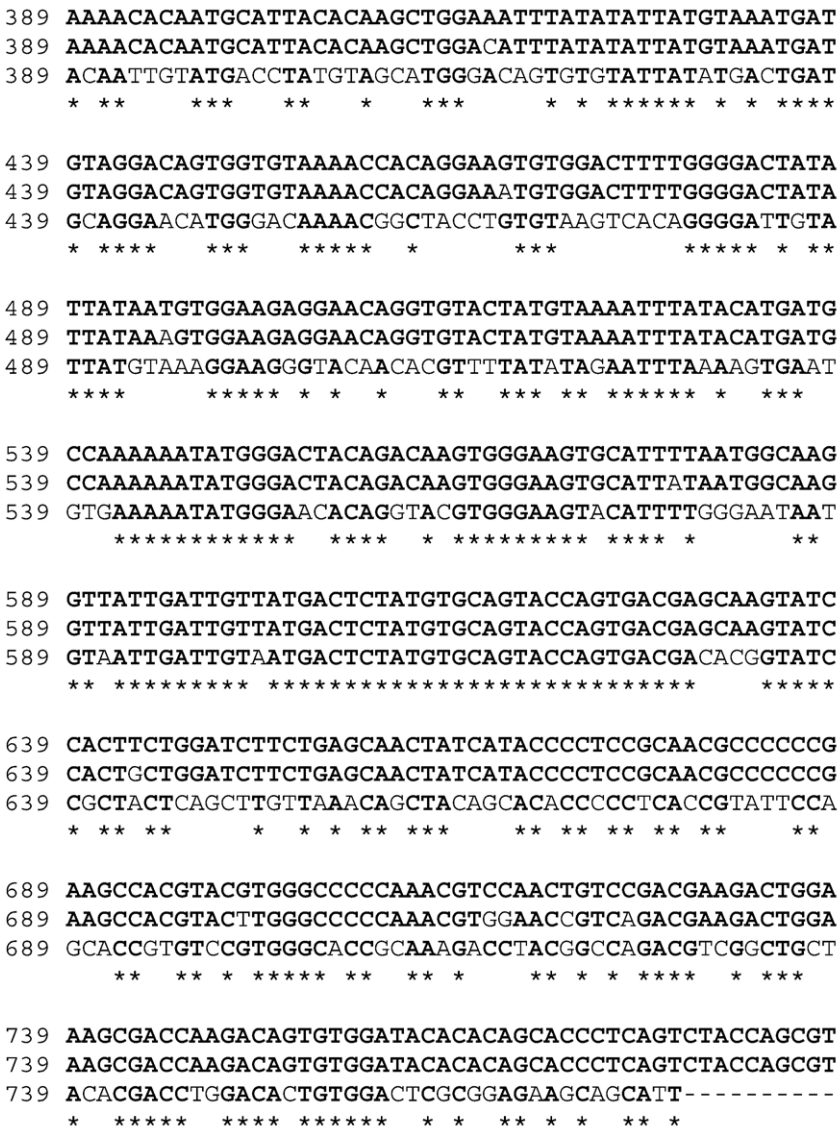

Fig. 1 (*continued*).

episomal HPV 59 per cell and could be induced to differentiate and produce infectious virus in a simple culture system that does not require rafts or engraftment into or onto mice (Lehr et al., 2003). During passage in vitro, we found evidence that HPV 59 sequences had integrated into cellular DNA. Thus, ERIN 59 cells could provide a unique model to study HPV 59 in both episomal and integrated forms on the same host background. Our studies focus on phenotypic and molecular differences in the virus and the host cell between HPV 59 in an episomal or integrated state.

Results

DNA sequence analysis of HPV 59 in ERIN 59 cells

DNA extracted from ERIN 59 cells was used in a PCR/reverse blot strip assay, which amplifies a portion of the L1 open reading frame (ORF). The PCR/reverse blot strip assay indicated the presence of HPV 59 DNA in ERIN 59 cells harvested at early and late passages (data not shown).

Published HPV 59 sequences have indicated that the E2 ORF contained an inverted portion in relationship to other HPV types between nucleotide (nt) positions 2970 through 3118 (Rho et al., 1994). It was suggested that this inversion could inactivate the transcriptional repressive activities of E2 in HPV 59.

In an attempt to verify this distinctive inversion, DNA was isolated from early passage ERIN 59 cells and the E2 gene was subsequently cloned and sequenced. The E2 DNA sequence of our HPV 59 isolate was very similar to the published HPV 59 sequence except in the region from nt 2970 through nt 3118, the region of the putative inversion (Fig. 1). The assigned GenBank accession number for the HPV 59 E2 sequence from ERIN 59 cells is AY923027.

```
789 GTCAGTGGACCACTGTGACAACCCAGTCGTCCGTTTGCATC--------C
789 GTCAGTGGACTACTGTGACAACCCAGTCGTCCGTTTGCATC--------C
779 ----GTGGACC----TGTCAACCCACTTCTCGG--TGCAGCTACACCTAC
        ******     ** ******* *  ** *  **** *        *

831 AGGCAACAACCCGCGACGGCACATCCCTTGCAGTAACACTACGCCTATAA
831 AGGCAACAACCCGCGACGGCACATCCCTTGCAGTAACACTACGCCTATAA
819 AGGCAACAACAAAAGACGGAAACTCTGTAGTGGTAACACTACGCCTATAA
    **********    ***** *  **  * *  ******************

881 TACACTTAAAAGGTGACAAAAATGGCCTTAAGTGTTTAAGGTATAGATT-
881 TACACTTAAAAGGTGACAAAAATGGCCTTAAGTGTTTAAGGTATAGATT-
869 TACATTTAAAAGGTGACAGAAACAGTTTAAAATGTTTACGGTACAGATTG
    **** ************ ***  *  * ** ****** **** *****

930 ----AAAAAAGGTACAATGGTTATTTGAAAATATTTCCTCTACCTGGCAT
930 ----AAGAAAAGTACACTGGTTATTTGAAAATATTTCCTCTACCTGGCAT
919 CGAAAACATAGCGACCA-----CTATAGAGATATATCATCCACCTGGCAT
        ** * *   **         * *  * **** ** ** *********

976 TGGACAGGAAACAGAGGATCAGCCAAAACAGGCATTTTAACATTAACATA
976 TGGACAGGAAACAGAGGATCAGCCAAAACAGGCATTTTAACATTAACATA
964 TGGACAGG---TGCAGGCAATGAAAAAACAGGAATACTGACTGTAACATA
    ********      ***    *  ******** **  * **  *******

1026 TACAAGCGAAACACAACGCAATGAATTTTTAGATACTGTAAAAATTCCTA
1026 TACAAGCGAAACACAACGCAATGAATTTTTAGATACTGTAAAAATTCCTA
1011 CCATAGTGAAACACAAAGAACAAAATTTTTAAATACTGTTGCAATTCCAG
         ** ********* * *   ******** *******   ******

1076 ATAGTGTACAAATACAAGTTGGGTATATGAGTGTGTAA
1076 ATAGTGTACAAATACATGTTGGGTATATGAGTGTGTAA
1061 ATAGTGTACAAATATTGGTGGGATACATGACAATGTAA
     ***************   ** ** ** ****   *****
```

Fig. 1 (*continued*).

At the amino acid level, the sequence of the E2 protein from our isolate was also similar to the published HPV 59 sequence except in the region corresponding to the amino acids encoded by nt 2970 through nt 3118 (Fig. 2). In contrast, the E2 DNA and protein sequences of our HPV 59 isolate shared a high degree of homology with those of HPV

```
                                                                                                  ↓
1 MQTVMDTLSQRLSVLQDQILEHYENDSKDINEHINYWKLVRMENVILFAARENNIHTLNHQVVPTFLVSKNKACEAIELQMALESLAQTEFKNEQWTMQE
1 MQTVMDTLSQRLSVLQDQILEHYENDSKDINEHINYWKLVRMENVILFAARENNIHTLNHQVVPTFLVSKNKACEAIELQSNRTSTVMPCFLKH--FLGA
1 MQTPKETLSERLSALQDKIIDHYENDSKDIDSQIQYWQLIRWENAIFFAAREHGIQTLNHQVVPAYNISKSKAHKAIELQMALQGLAQSAYKTEDWTLQD
  ***   *** *** *** *  *********   * ** * * ** * *****  * ********    ** **  *****

                    ↓
101 TCQELWQTAP-KKCFKKQGITVEV-RFDCSKENTMHYTSWKFIYYVNDVGQWCKTTGSVDFWGLYYNVEEEQVYYVKFIHDAKKYGTTDKWEVHFNGKVI
 99 VCHSSWHVSCIVHCSFLNSVCAKLSNAICSKENTMHYTSWTFIYYVNDVGQWCKTTGNVDFWGLYYKVEEEQVYYVKFIHDAKKYGTTDKWEVHYNGKVI
101 TCEELWNTEP-THCFKKGGQTVQV-YFDGNKDNCMTYVAWDSVYYMTDAGTWDKTATCVSHRGLYYVKEGYNTFYIEFKSECEKYGNTGTWEVHFGNNVI
     *   *       *               * * * *   **  * * * **   *   **** *     *  *     *** *  ****    **

199 DCYDSMCSTSDEQVSTSGSSEQLSYPSATPPEATYVGPQTSNCPTKTGKRPRQCGYTQHPQSTSVSVDHCD--NPVV--RLHPGNNPRRHIPCSNTTPII
199 DCYDSMCSTSDEQVSTAGSSEQLSYPSATPPEATYLGPQTWNRQTKTGKRPRQCGYTQHPQSTSVSVDYCD--NPVV--RLHPGNNPRRHIPCSNTTPII
199 DCNDSMCSTSDDTVSATQLVKQLQHTPSPYSSTVSVGTAKTYGQTSAATRPGHCGLAEK--------QHCGPVNPLLGAATPTGNNKRRKLCSGNTTPII
    ** ********  **      **           *       *    **  **             *   **        *** **     ******

295 HLKGDKNGLKCLRYRLKKVQWLFENISSTWHWTGNRGSAKTGILTLTYTSETQRNEFLDTVKIPNSVQIQVGYMSV
295 HLKGDKNGLKCLRYRLRKVHWLFENISSTWHWTGNRGSAKTGILTLTYTSETQRNEFLDTVKIPNSVQIHVGYMSV
291 HLKGDRNSLKCLRYRLRKHSDHYRDISSTWHWTG-AGNEKTGILTVTYHSETQRTKFLNTVAIPDSVQILVGYMTM
    ***** * ******** *       *********  *  ****** ** *****  ** ** ** **** ****
```

Fig. 2. Alignment of E2 proteins based on the DNA sequence from ERIN59 cells (top sequence), the protein based on the published HPV 59 DNA sequence (middle sequence), and the E2 protein based on published HPV 18 DNA sequence (bottom sequence). Amino acids are indicated by single letter designation, and the number of the amino acid within the E2 protein is shown on the left side of the figure. Bold lettering indicates amino acids matching with the sequence from ERIN59 cells. Star symbols (*) indicate matching amino acids for all three sequences. The sequence between the methionine (M) at position 81 (arrow over the residue) and the aspartic acid (D) at position 126 (arrow over the residue) correspond to the putative inversion error in the published HPV 59 sequence.

18, even in the area of the putative inversion (Figs. 1 and 2). These data suggest that, in contrast to the published HPV 59 E2 sequence (Rho et al., 1994), the HPV present in ERIN 59 cells does not contain an inversion within E2.

Morphology, growth requirements, and tumorigenicity of late passage ERIN 59 cells

ERIN 59 cells were originally derived from an HPV 59-infected foreskin xenograft grown in an athymic mouse (Lehr et al., 2003). Initially, early passage ERIN 59 cells were grown in complete F medium and required the presence of mitomycin-treated J2 fibroblasts (Flores et al., 1999). Compared to primary human keratinocytes (PHKs) (Fig. 3, panel A), early passage ERIN 59 cells were smaller and pleomorphic (Fig. 3, panel B). After approximately 50 passages, ERIN 59 cells could be grown in complete F medium without fibroblasts, had larger and atypical nuclei, with numerous multinucleate cells and mitotic figures (Fig. 3, panel C). Attempts to grow early passage cells without fibroblasts were unsuccessful.

Soft agar colony formation assays were performed to assess the anchorage-independent growth capacity of early passage ERIN 59 cells (passage 13) and late passage ERIN 59 cells (passage 137) (Fig. 4). PHKs did not form colonies in soft agar (Fig. 4, panels A and D). Early passage ERIN 59 cells formed an average of 0.7 colonies per high power field (Fig. 4, panels B and D). In contrast, late passage ERIN 59 cells formed an average of 14.0 colonies per high power field (Fig. 4, panels C and D).

Both early passage ERIN 59 cells (passage 12) and late passage ERIN 59 cells (passage 63 and passage 95) failed to develop tumors in athymic mice after subcutaneous injection. Four injection sites were observed from each passage of cells analyzed. In contrast, HeLa cells generated robust subcutaneous tumors under the same conditions (data not shown).

Late passage ERIN 59 cells contain integrated HPV 59, disrupted within the E2 ORF

The tyramide-amplified DNA in situ hybridization method provides evidence regarding the physical state of HPV viral DNA (Cooper et al., 1991; Evans and Cooper, 2004; Evans et al., 2002; Kerstens et al., 1995; Sano et al., 1998). Cells containing episomal DNA display a diffuse, whole nuclear signal while cells with integrated viral DNA show punctate signals within nuclei. Therefore, the physical state of HPV 59 in late passage ERIN 59 cells was analyzed using tyramide-amplified DNA in situ hybridization. As a negative control, an assay of an uninfected foreskin xenograft grown in an athymic mouse was performed, yielding no signal (Fig. 5, panels A and B). As a positive control for episomal HPV 59 infection, an assay of an HPV 59-infected foreskin xenograft was performed. A diffuse, whole nuclear signal was detected in the most differentiated cells of the infected xenograft (Fig. 5, panels C and D). Early passage ERIN 59 cells were previously shown to contain episomal HPV 59 (Lehr et al., 2003). Analysis of early passage ERIN 59 cells (passage 12), grown under differentiation inducing conditions, revealed a diffuse, whole nuclear signal consistent with episomal DNA (Fig. 5, panels E and F). In contrast, analysis of late passage ERIN 59 cells grown under similar conditions revealed punctate signals consistent with integrated HPV 59 (Fig. 5, panels G and H). The greater intensity of the staining seen in panels D and F compared to panel H may reflect the amplification of HPV 59 DNA by vegetative replication in these cells following growth under differentiation-inducing conditions. Hematoxylin- and eosin-stained sections are shown as a reference for size and density of nuclei (Fig. 5, panels A, C, E, and G).

As indicated above, early passage ERIN 59 cells contain approximately 50 copies of episomal HPV 59 per cell (Lehr et al., 2003). To further determine the form and copy number of the viral genome in late passage (passage 142) ERIN 59 cells, Southern blot analysis was performed. The HPV 59 radiolabeled DNA hybridized with high molecular weight uncut late passage ERIN 59 DNA (Fig. 6, lane 6), consistent with integrated or multimeric viral DNA. To distinguish between these two alternatives, ERIN 59 DNA was cut with *Bam*HI, which cleaves HPV 59 once. If the genome is multimeric and/or episomal, *Bam*HI digestion should yield HPV DNA migrating at the position of full-length HPV 59 8 kb DNA. Instead, two bands were seen, at approximately 18 and 6 kb, consistent with an integrated viral form at a single locus (Fig. 6, lane 4). The absence of an 8-kb HPV band in the *Bam*HI digested DNA further suggests that the integrant is not present in a head-to-tail multimeric form. To substantiate that the viral genome was integrated at a single site, ERIN59 DNA was cleaved with *Hin*dIII, which does not cleave HPV 59 DNA. The HPV 59 whole genomic probe hybridized with *Hin*dIII-digested DNA as a single band of approximately 19 kb (Fig. 6, lane 5). Incomplete *Hin*dIII digestion was responsible for the diffuse signal at approximately 23 kb, as a repeat of the Southern blot with longer *Hin*dIII digestion produced only a single band at 19 kb (data not shown). Thus, only a single integration site was detected. Copy number controls indicated that the viral copy number in the late passage ERIN 59 cells was approximately one copy per cell (Fig. 6, lanes 1–3).

Lastly, limiting cycle PCR was performed on DNA from early and late passage ERIN 59 cells. In early passage cells, amplimers from viral genes E6, E7, E1, L1, and E2 were visualized after 20 cycles of amplification (Fig. 7, rows labeled “E”). In contrast, amplimers from viral genes E6, E7, E1, and L1 were visualized only after 26 cycles of amplification using equivalent

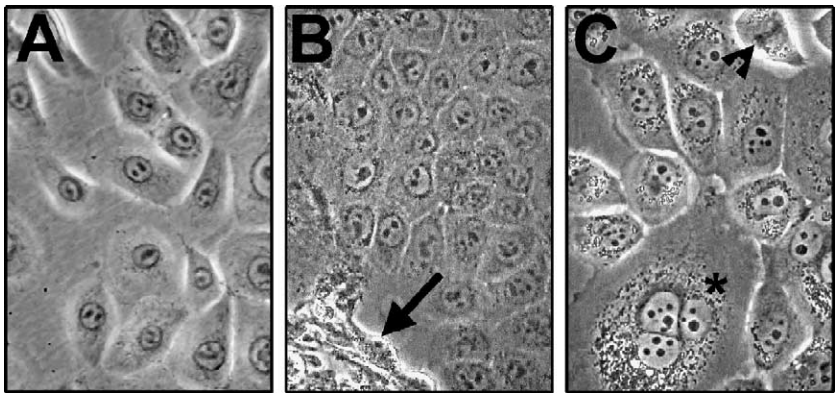

Fig. 3. Phase contrast micrographs of cells grown as monolayers. (A) PHKs; (B) early passage (passage 8) ERIN 59 cells. Arrow indicates J2 feeder fibroblasts. (C) Late passage (passage 98) ERIN 59 cells. Arrowhead indicates a mitotic figure. Asterisk indicates a multinucleate cell. Original magnification: 200×.

quantities of whole genomic DNA from late passage ERIN 59 cells (Fig. 7, rows labeled "L"). In addition, although abundant E2 amplimers were obtained from early passage ERIN 59 cellular DNA, E2 could not be amplified by PCR from late passage ERIN 59 cell DNA, even after 35 cycles (data not shown). Failure to amplify E2 sequences is consistent with disruption of the E2 ORF upon integration.

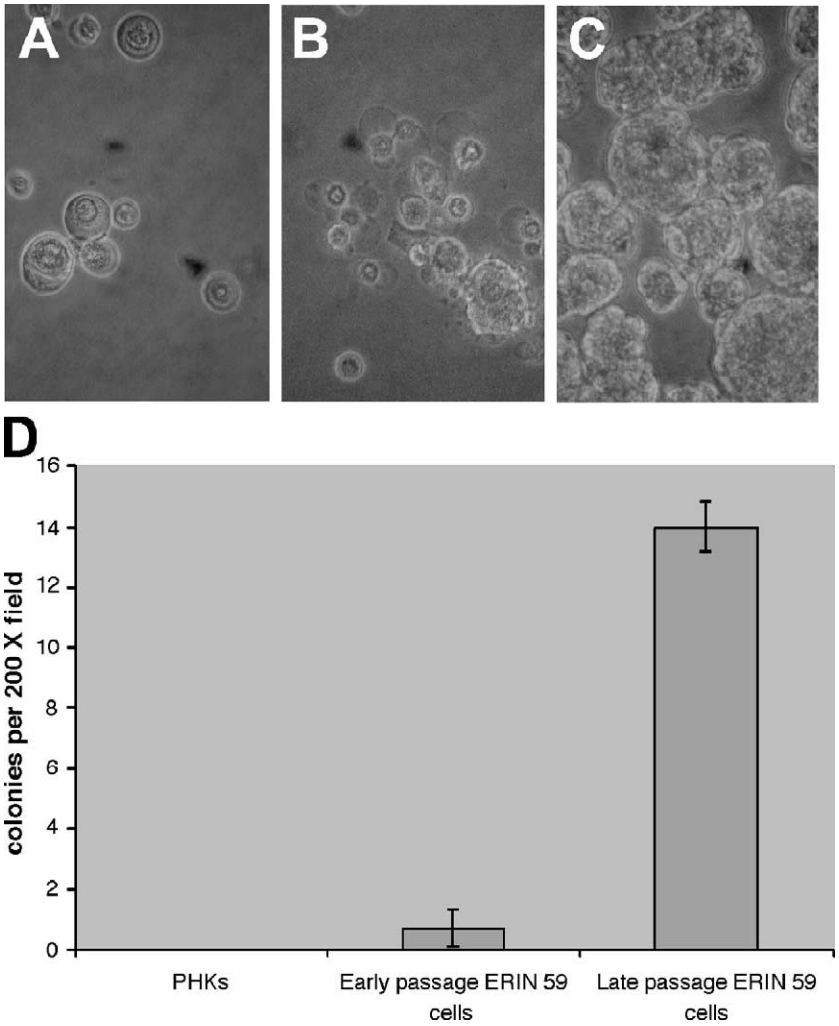

Fig. 4. Analysis of soft agar colonies. (A, B, and C) Phase contrast micrographs of soft agar colonies of PHKs (A), early passage ERIN 59 cells (B), and late passage ERIN 59 cells (C). Original magnification: 200×. (D) Graph indicating the average number of soft agar colonies per high power field (hpf) for early and late passage ERIN 59 cells. Standard deviations reflect the differences between three experimental replicates.

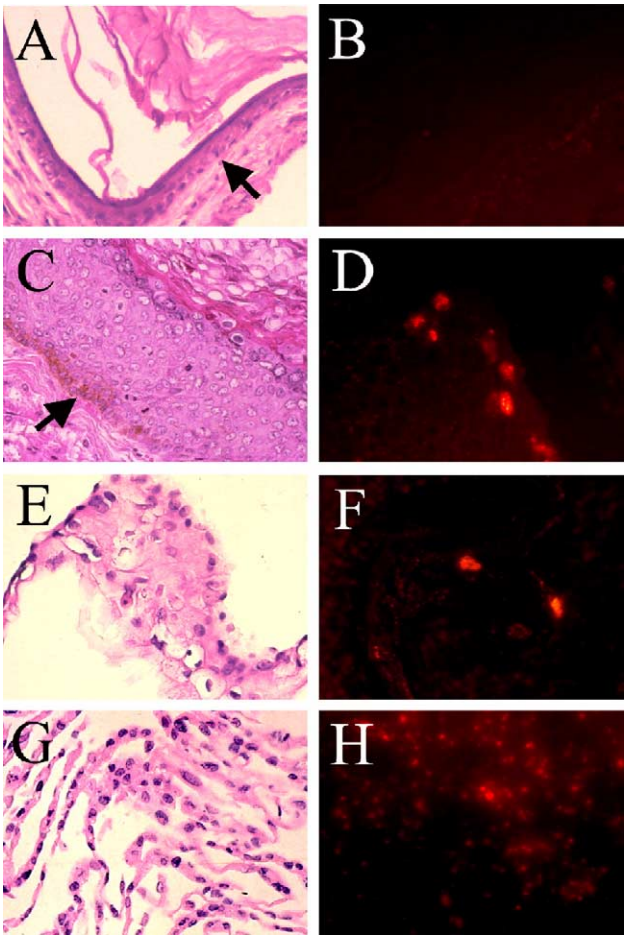

Fig. 5. Histologic and DNA in situ hybridization analysis to detect HPV 59 sequences in foreskin xenografts and in cells grown in complete F medium with 2 mM calcium chloride to induce differentiation. Hematoxylin and eosin (H&E) section (A) and DNA in situ analysis (B) of uninfected foreskin xenograft. H&E section (C) and DNA in situ analysis (D) of HPV 59-infected foreskin xenograft. H&E section (E) and DNA in situ analysis (F) of early passage ERIN 59 cells. H&E section (G) and DNA in situ analysis (H) of late passage ERIN 59 cells. Arrows in panels A and C indicate the basal cell layer in the foreskin xenografts. Original magnification: 400×.

Late passage ERIN 59 cells express high levels of an integration-derived HPV oncogene-containing transcript

An integration-derived HPV 59 oncogene transcript was detected in late passage ERIN 59 cells using analysis of papillomavirus oncogene transcripts (APOT) (Klaes et al., 1999). This transcript encodes the complete E6 and E7 ORFs, followed by 16 nucleotides (nts) of E1 spliced to the 3′ end of the E1 gene at base pair position 2695. The splice is upstream of the start of E2 at nt 2736. The E2 gene is intact through nt 3351 of HPV 59, where the viral sequence abruptly ends and is followed by 22 nts of presumably cellular encoded transcript just prior to the polyA$^+$ tail (Fig. 8). This was the only transcript recovered in multiple independent APOT analyses and is therefore likely to be the predominant oncogene transcript. No E6 splice variants were recovered. The HPV 59 sequence at nt 3351 does not resemble a consensus splice donor site. Therefore, it is unlikely that the switch from HPV 59 E2 sequence to cellular sequence represents a splice donor/acceptor site. A single-base polyadenylation signal variant, AATAGA, was located 19 base pairs upstream of the polyadenylation site within the cellular encoded sequence. Therefore, it is likely that the E2 gene is disrupted by integration at nt 3351 and the integration-derived transcript reflects the native junction between virus and host DNA.

As indicated above, the transcript contained nt 2736 through nt 3351 of the E2 ORF. The complementary E2 sequence of the transcript matched that of the E2 sequence of our HPV 59 isolate, including the region from nt 2970 through nt 3118, (the region of the putative inversion). The viral genes E6 and E7 were also sequenced from the integration-derived transcript and showed high homology to published HPV 59 sequences (data not shown).

Because the transcript contained only 22 nts of cellular encoded message, we were unable to determine the cellular integration loci based on the APOT analysis as a BLAST search retrieved numerous regions within the human genome having homology to this sequence. We are therefore currently employing other methods to determine the precise integration locus. These future studies will also allow confirmation that the viral/cellular junction in this transcript is not due to splicing.

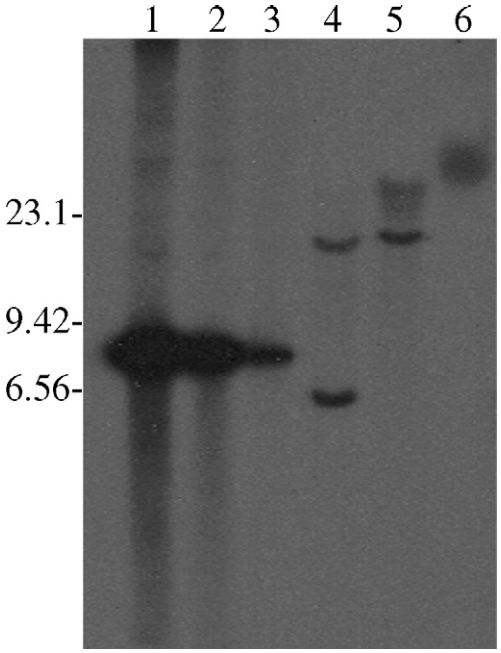

Fig. 6. Southern blot analysis of late passage (passage 142) ERIN 59 cells. Copy number controls, as indicated in the text, are shown in lanes 1 (approximately 9.6 copies per cell), 2 (approximately 1.9 copies per cell), and 3 (approximately 1.0 copy per cell). DNA from late passage ERIN 59 cells was digested with *Bam*HI (lane 4), *Hin*dIII (lane 5), or no enzyme (lane 6). Molecular markers (in kb) are indicated on the left side of the figure.

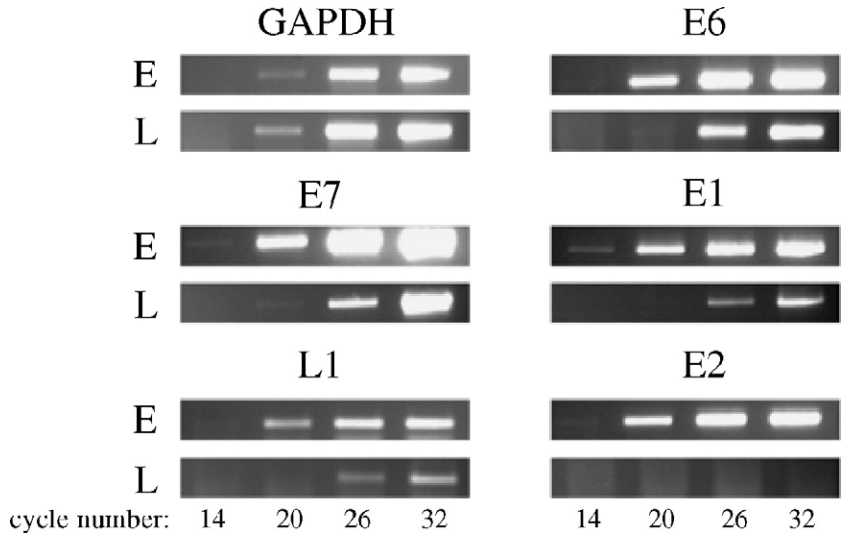

Fig. 7. Limiting cycle PCR to amplify HPV 59 genes. Rows labeled "E": PCR using DNA from early passage (passage 13) ERIN 59 cells. Rows labeled "L": PCR using DNA from late passage (passage 63) ERIN 59 cells. The primer sets used in each PCR are indicated at the top of each set of rows. GAPDH was used as an internal control for balanced DNA content. Cycle numbers are indicated at the bottom of the figure (see text for explanation).

To compare the relative abundance of oncogene-encoding transcripts in early and late passage ERIN 59 cells, limiting cycle RT-PCR was performed using RNA from these cells (Fig. 9). E6/E7-encoding transcripts were expressed at similar levels in cells from both passages, despite a higher DNA copy number in early passage cells. As expected, transcripts potentially encoding the complete E2 ORF were not detected by RT-PCR in late passage ERIN 59 cells.

Late passage ERIN 59 cells have a decreased capacity to differentiate

Some degree of differentiation is necessary for HPV virus production. Yet failure of differentiation or markedly aberrant differentiation is a characteristic of tumor cells. Therefore, studies were conducted to characterize the differentiation capacity of early and late passage ERIN 59 cells. To detect cellular transcripts encoding involucrin (a cornified cell envelope protein expressed in differentiated keratinocytes), limiting cycle RT-PCR was performed using RNA from PHKs (Fig. 10, rows labeled "P"), and from early passage ERIN 59 cells (Fig. 10, rows labeled "E") and late passage ERIN 59 cells (Fig. 10, rows labeled "L") following 7 days of stimulation with 2 mM calcium chloride to induce differentiation. All differentiation studies were conducted on cells adherent to plastic tissue culture flasks. Calcium chloride was added to the regular cell culture medium. Upon calcium-induced differentiation, transcripts potentially encoding involucrin were detected in early passage ERIN 59 cells at levels comparable to PHKs, while late passage ERIN 59 cells expressed lower levels of involucrin transcripts (Fig. 10, middle group of rows). Early passage ERIN 59 cells also produced abundant levels of transcripts encoding the L1 major capsid protein upon calcium-induced differentiation (Fig. 10, right group of rows). Late passage ERIN 59 cells produced fewer L1 transcripts than early passage ERIN 59 cells under the same conditions.

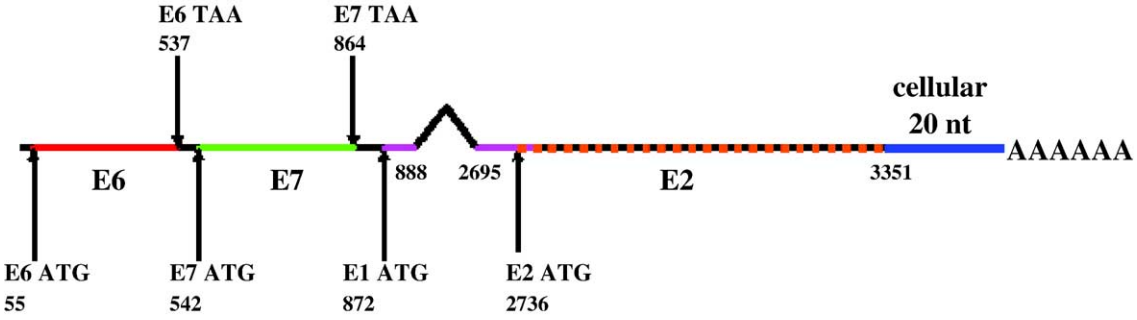

Fig. 8. Diagram representing E6 and E7 oncogene encoding viral–cellular fusion transcript detected in late passage ERIN 59 cells. Numbers under the sequence indicate the positions of splice donor/acceptor nucleotides. The HPV 59 E6 ORF spans from nt 55 through nt 537. The HPV 59 E7 ORF spans from nt 542 through nt 864. HPV 59 E2 spans from nt 2736 through nt 3848. E2 is interrupted in this transcript at nt 3351, and is immediately followed by 22 nts of non-HPV, presumably cellular, encoded transcript immediately preceding the polyA$^+$ tail.

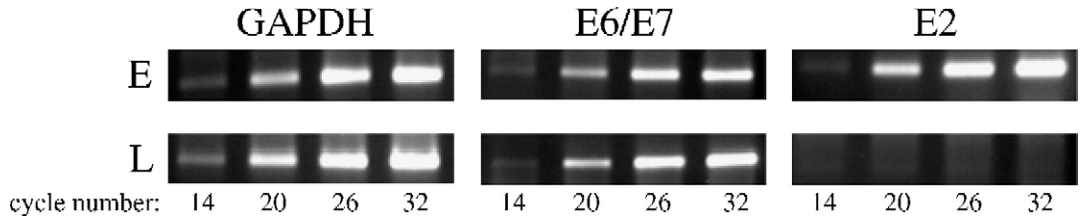

Fig. 9. Limiting cycle RT-PCR to detect HPV 59 transcripts. Rows labeled "E": RT-PCR using RNA from early passage ERIN 59 cells (passage 9). Rows labeled "L": RT-PCR using RNA from late passage ERIN 59 cells (passage 73). The primer sets used in each RT-PCR are indicated at the top of each set of rows. GAPDH was used as an internal control for balanced DNA content. Cycle numbers are indicated at the bottom of the figure (see text for explanation).

Histologic and immunohistochemical analysis of these cells, stimulated to differentiate with calcium chloride, was also performed to look for evidence of differentiation (Fig. 11). PHKs and early passage ERIN 59 cells grown as submerged cultures showed a limited degree of stratification (three to four cells in thickness), while late passage ERIN 59 cells were only one to two cells thick. Immunohistochemical analysis was performed to detect involucrin and L1 proteins. Involucrin was detected in abundance in PHKs and early passage ERIN 59 cells, but not in late passage ERIN 59 cells. The L1 major capsid protein was detected in early passage ERIN 59 cells as a nuclear signal (Fig. 11, panel H), but was not detected in late passage ERIN 59 cells (Fig. 11, panel I). Analysis of cells with preimmune rabbit serum yielded no appreciable signals (data not shown).

Discussion

ERIN 59 cells are immortalized human foreskin keratinocytes derived from an HPV 59-infected foreskin xenograft grown in an athymic mouse (Lehr et al., 2003). HPV 59 is a high-risk type closely related to HPV 18, sharing a 71% overall sequence homology (Rho et al., 1994, 1996). The ERIN 59 cell line provides a valuable model to study the progression of HPV-induced disease from episomal viral infection, in which infectious virions can be produced to integration and associated neoplastic changes.

The previously published sequence of HPV 59 indicated a large inversion within the E2 ORF. It has been suggested that this inversion may obliterate the transcriptional repressive function of E2 in HPV 59 infection. However, no portion of the E2 ORF was inverted in our HPV 59 isolate compared to HPV 18. Rather, E2 was closely homologous with the HPV 18 E2 sequence at the DNA and protein level. It is possible that the published HPV 59 isolate may in fact contain this inversion within E2. Another possible explanation, suggested by the authors of the published sequence, is that an error occurred during the alignment process (Rho et al., 1994). Regardless of the reason for the disparity, our HPV 59 isolate is homologous to HPV 18 throughout the E2 ORF at the nucleotide and amino acid level. These results demonstrate an even closer overall homology between HPV 59 and HPV 18 than was previously known. We concluded that our HPV 59 isolate contained no inversion in the E2 region.

The results also suggest that the transcriptional repressive function ascribed to the E2 gene in other high-risk HPV types is conserved in HPV 59 E2 (Bernard et al., 1989; Demeret et al., 1997; Dowhanick et al., 1995; McBride and Howley, 1991; Nishimura et al., 2000; Thierry and Howley, 1991). It is worth noting that E2 did not repress HPV transcription of E6 and E7 in W12 cells containing episomal HPV 16 (Bechtold et al., 2003). However, in S12 cells, an isolate of W12 cells containing integrated HPV 16, ectopic expression of E2 elicited strong repression of E6 and E7 transcription (Bechtold et al., 2003).

Disruption within the E2 ORF is frequently observed in cervical malignancies, and the disruption of the E2-dependent negative feedback controlling E6/E7 transcription is considered a selective event in tumor development and progression (zur Hausen, 1991; Romanczuk and Howley, 1992). In late passage ERIN 59 cells, E2 was found to be disrupted at the DNA level. Transcriptional analyses revealed that an oncogene-containing viral transcript also contained E2 sequences, truncated at base pair position

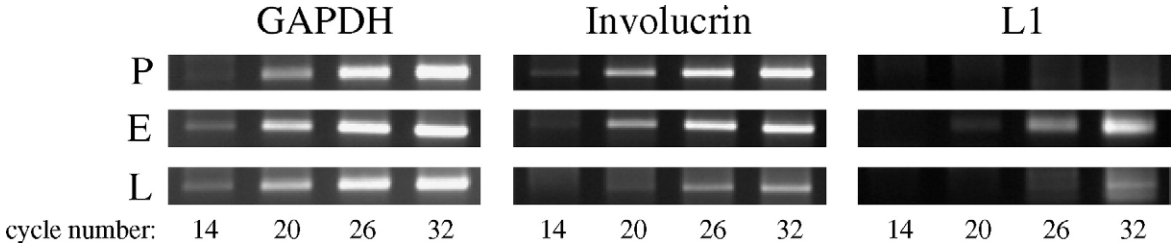

Fig. 10. Limiting cycle RT-PCR for detection of differentiation-specific transcripts using RNA from cells grown in complete F medium containing 2 mM calcium chloride. Rows labeled "P": PHKs. Rows labeled "E": early passage ERIN 59 cells (passage 12). Rows labeled "L": late passage ERIN 59 cells (passage 100). GAPDH was used as an internal control for balanced RNA levels. Primer sets are indicated at the top of each set of rows. Cycle number is indicated at the bottom of the figure.

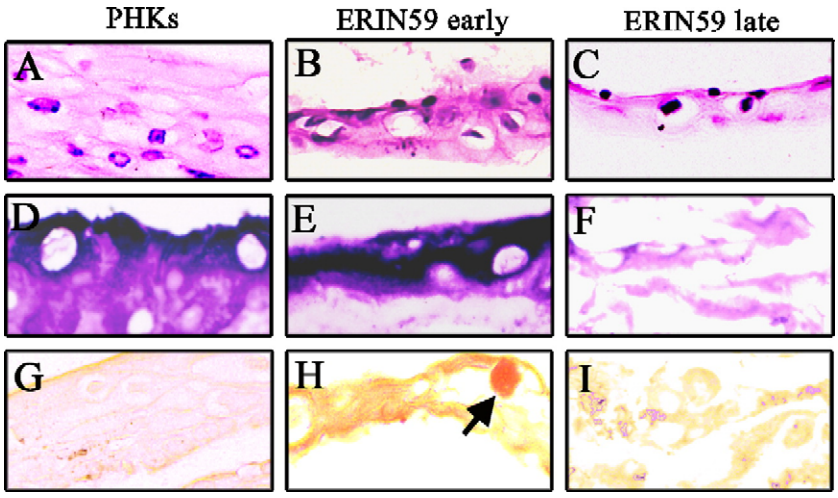

Fig. 11. Histology and immunohistochemical analysis of PHKs (A, D, and G), early passage (passage 12) ERIN 59 cells (B, E, and H) and late passage (passage 52) ERIN 59 cells (C, F, and I) grown submerged in complete F medium containing 2 mM calcium chloride. Histology is indicated in hematoxylin and eosin-stained sections (A, B, and C). Immunohistochemical analysis to detect involucrin (D, E, and F) and the L1 major capsid protein (G, H, and I). The arrow in panel H indicates the nucleus of a cell that stained positive for L1 protein in early passage ERIN59 cells. Original magnification: 400×.

3351, and fused to cellular sequences. Therefore, in late passage ERIN 59 cells, an E2 protein encoded from this message would be missing the DNA binding portion, thus abrogating a transcriptional repressive function (Dowhanick et al., 1995; Gillitzer et al., 2000; McBride and Howley, 1991).

As expected in the case of abrogated E2 function, the production of E6 and E7 transcripts was high in late passage cells in spite of a lower viral copy number compared to early passage cells. This has been previously observed for HPV 16-immortalized cervical keratinocytes, in which a selective growth advantage was noted for clones containing integrated HPV sequences (Jeon et al., 1995). In spite of lower HPV copy number in these clones, the expression of E7 exceeded that in clones with episomal HPV 16, most likely a result of loss of E2-mediated repression of E6/E7 transcription in the clones with integrated HPV. In the case of ERIN59 cells, this suggests that the loss of E2 in late passage cells has resulted in a lack of E2-mediated transcriptional repression and provides additional evidence that HPV 59 E2 acts as a transcriptional repressor to down-regulate transcription of E6 and E7 oncogenes.

Low-grade HPV-associated dysplastic lesions and cell lines derived from these lesions retain some degree of differentiation and the potential to produce infectious virus (De Geest et al., 1993; Fichorova et al., 1997; Sterling et al., 1993). In contrast, high-grade lesions and carcinomas differentiate poorly and are devoid of virus production. Poor or absent differentiation is a feature of cervical cancers (Robboy et al., 2002). While early passage ERIN 59 cells showed a degree of differentiation in culture when stimulated with calcium, late passage ERIN 59 cells showed much less differentiation under the same conditions. Thus, this progression towards failure to differentiate was recapitulated in ERIN 59 cells, suggesting that these cells represent a useful model of HPV 59-induced neoplasia.

Anchorage-independent growth is generally accepted as an in vitro property of neoplastic cells. Late passage ERIN 59 cells had an increased capacity for anchorage-independent growth compared to early passage ERIN 59 cells. This progression towards increased capacity for anchorage-independent growth further suggests that these cells represent a useful model of HPV 59-induced neoplasia.

Consistent with these observations, late passage ERIN 59 cells exhibited some phenotypic traits associated with neoplasia that were not evident in early passage cells. Such traits included the ability to grow in the absence of fibroblast feeders, enhanced nuclear atypia, increased capacity for anchorage-independent growth, and reduced differentiation capacity. Primary cells generally require exogenous growth factors for continuous proliferation (Herlyn et al., 1990). However, cell lines developed from transformed cells or carcinomas as diverse as tracheal epithelium, bladder, colon, ovary, and cervix are able to proliferate after a short adaptation period in medium depleted of growth factors. Additionally, with time in culture, cells show a reduction of their growth requirements (Aaronson, 1991; Herlyn et al., 1990). Thus, the process of in vitro passaging could, in part, account for the decreased growth requirements and increased nuclear atypia in late passage ERIN 59 cells, which prompted us to begin these studies. This is even more probable when taking into account the continuous exposure to high levels of E6 and E7 oncogenes throughout in vitro passaging.

A second contributing factor to the more malignant phenotype observed in late passage ERIN 59 cells is the physical state of the HPV 59 genome. Premalignant lesions of the cervix typically contain HPV predominantly in an episomal form, while cervical carcinomas usually contain integrated HPV sequences (Badaracco et al., 2002; Das et al., 1992; Evans et al., 2002; Gross and Pfister, 2004; Hernadi et al., 2004; Hopman et al., 2004; Hudelist et al., 2004; Lizard et al., 1998). Therefore, it follows that the

phenotype of cells with integrated HPV DNA would exhibit a more neoplastic phenotype than cells with episomal HPV DNA. Integration of HPV sequences into the human genome has been shown to enhance the stability of E6/E7-encoding transcripts, providing a potential means of optimizing the effects of these oncogenes on cellular growth (Jeon and Lambert, 1995). HPV 59 is a close relative of HPV 18. It has been suggested that HPV 18 may possess an enhanced ability to integrate into the host genome at an early point in infection compared to HPV 16 (Badaracco et al., 2002).

It has recently been shown that the integration of high-risk HPV is associated with numerous changes in cellular gene expression (Alazawi et al., 2002) and with acquisition of high-level chromosomal instability (Pett et al., 2004). Thus, the integrated state of the viral genome in late passage ERIN 59 cells might contribute to an increasingly unstable genome allowing the acquisition of chromosomal abnormalities associated with neoplastic progression. Alternatively, the presence of integrated viral DNA may simply reflect the increase in genomic instability induced by prolonged exposure to E6 and E7.

While HPV infection and neoplastic progression has been most widely studied in cervical cancer, HPV also plays an important role in carcinogenesis of the vagina (Barzon et al., 2002; Daling et al., 2002; Logani et al., 2003; van Beurden et al., 1998) and penis (Bezerra et al., 2001; Dillner et al., 2000; Gross and Pfister, 2004). As indicated above, ERIN 59 cells were derived from foreskin keratinocytes. In spite of their different cellular origin, ERIN 59 cells share many common phenotypic features of neoplasia with W12 and UT-DEC-1 cells, derived from cervical and vaginal keratinocytes, respectively. Notably, all three cell lines contained episomal HPV at early passage and were superseded by cells containing integrated HPV during passage in vitro.

For all three of these cell lines, early passage cells provide a model for the study of episomal infection and the viral life cycle. Virus particles have been produced from early passages of both the W12 cell line and ERIN 59 cell line (Flores and Lambert, 1997; Lehr et al., 2003). These cell lines and UT-DEC-1 cells have exhibited progressive changes towards a malignant phenotype in later passages (Auvinen et al., 1998; Pett et al., 2004). Thus, these cell lines each serve as important models of HPV-induced neoplastic progression in different genital keratinocytes.

Comparisons among these cell lines will help elucidate common features of HPV-induced neoplastic progression at different sites susceptible to HPV infection and disease. Contrasting observations between these cell lines might also shed light on how different HPV types affect progression of HPV-induced neoplasia. Also, it is important to examine differences between HPV infection involving various host genetic backgrounds, and different anatomical locations of infection.

Methods

Cell culture

PHKs derived from foreskin were grown in Epilife growth media (Cascade Biologics, Inc. Portland, OR). Early passage ERIN 59 cells were plated onto J2 feeder fibroblasts (treated with mitomycin C, 4 μg/mL for 16 h) in incomplete F medium. Medium was changed to complete F medium after 24 h. Complete F medium is identical to incomplete F but with epidermal growth factor (Sigma, St. Louis, MO) supplement added at a final concentration of 10 ng/mL. Late passage ERIN 59 cells were grown in complete F medium. All cells were maintained in a 5% CO_2 incubator at 37 °C. All cells were divided every 4–5 days.

Cloning and sequence analysis of viral gene E2

The HPV 59 E2 ORF (nts 2736 through 3848) was amplified by PCR from whole genomic DNA isolated from early passage ERIN 59 cells using the following primers: (Forward) 5′-AGATCTAGGAAGATGCAGACAGTGATG-GAC-3′, (Reverse) 5′-GCGGCCGCCAACCATTACA-CACTCATATAC-3′ with the following cycling parameters; 94 °C for two min, followed by 30 cycles of 94 °C for 45 s, 55 °C for 45 s, and 72 °C for 60 s, followed by a single 72 °C incubation for 5 min. The 1124 base pair amplimer (nts 2730 through 3854) was cloned into PCR-II-TOPO (Invitrogen Corp., Grand Island, NY) and subjected to single pass primer extension sequencing (ACGT, Inc., Wheeling, IL). Portions of the sequence were independently verified by single pass primer extension analysis (ACGT, Inc.) using internal primers at E2 base pair position 2843 5′-TTGGAAACTG-GTGCGTATGG-3′ and at E2 base pair position 3376 5′-GTGGATACTTGCTCGTCACT-3′.

Growth in athymic mice

Early passage ERIN 59 cells (passage 12) and late passage ERIN 59 cells (passage 63 and passage 95) were trypsinized, resuspended in complete F medium, washed in PBS, then resuspended in PBS at 10^6 cells per 200 μL PBS. The cell slurry was injected subcutaneously in the axillary region of athymic mice at 200 μL/injection site, with four injection sites for each cell passage (passages 12, 63, and 95). Injection sites were observed for tumor formation for 2 months. Similarly prepared HeLa cells were used as a positive control. PBS alone was used as a negative control.

Colony formation in soft agar

PHKs, early passage ERIN 59 cells (passage 13) and late passage ERIN 59 cells (passage 137) were trypsinized, counted by trypan blue exclusion assay, and resuspended in medium containing 0.3% melted SeaPlaque agarose (Cambrex Bio Science Rockland, Inc. Rockland, ME). Media

used were Epilife for PHKs and complete F for early passage ERIN 59 cells and late passage ERIN 59 cells. Aliquots of 2 mL containing 5×10^4 cells were plated in triplicate over a 2-mL base layer of solidified 0.6% agarose-containing medium. Colonies per high power field were counted by two observers following 5 days of incubation in a humidified 5% CO_2 incubator at 37 °C. Ten fields were counted for each experimental group. Standard deviations reflect the differences between three experimental replicates.

PCR/reverse blot strip assay and Southern blot analysis

DNA was isolated from late passage (passage 142) ERIN 59 cells using the genomic DNA isolation from cultured cells protocol (GerardBiotech, Oxford, OH). DNA concentration was determined by spectrophotometry. The presence of high molecular weight DNA was established by agarose gel electrophoresis followed by staining with ethidium bromide. PCR and reverse blot strip assay (Roche Molecular Diagnostics, Carmel, IN) was performed as previously described to confirm the presence of HPV 59 sequences (Bryan et al., 2000).

For the Southern blot, 20 μg of genomic DNA from passage 142 ERIN 59 cells (prepared as above described) was digested with *Bam*HI, *Hin*dIII, or no added restriction enzyme for 2 h at 37 °C. Digested DNA was separated by 0.8% agarose gel and alkaline transferred to nylon membrane (Hybond-N+, Amersham Bioscience, Piscataway, NJ). To prepare the probe for Southern blot analysis, the 8-kb genomic HPV 59 sequence was excised from the pCR-XL-TOPO vector by endonuclease digestion using *Bam*HI, purified from an agarose gel and labeled with [α-^{32}P]dATP using the Random Primed Labeling Kit (Roche Molecular Diagnostics). Labeled probe was purified with Microspin G-50 Column (Amersham Bioscience). The membrane was prehybridized with Expresshyb Solution (BD Bioscience Clontech, San Jose, CA) for 2 h at 60 °C and subsequently hybridized with labeled probe diluted in Expresshyb solution for 2 h at 60 °C. After hybridization, the membrane was washed with 2× SSC, 0.05% SDS at room temperature for 30 min with several changes of the solution and then 0.1× SSC, 0.1% SDS at 50 °C for 30 min. The membrane was then exposed to X-ray film (X-OMAT AR film, Kodak, Rochester, NY). For copy number estimation, a total of 500 pg (approximately 9.6 copies per cell), 200 pg (approximately 1.9 copies per cell), or 50 pg (approximately 1.0 copies per cell) linearized HPV 59 whole genomic DNA were applied to the agarose gel.

Limiting cycle PCR

Confluent early passage ERIN 59 cells (passage 13) and late passage ERIN 59 cells (passage 63) were washed with PBS. Proteinase K (Qiagen, Inc., Valencia, CA) was added directly to the adherent cells followed by incubation at 55 °C for 30 min. DNA was harvested using the QIAamp DNA Mini Kit (Qiagen). PCR was performed using 1.2 μg total DNA using SuperTaq (Ambion, Inc., Austin, TX). Primers used are indicated in Table 1. PCR was performed as follows: 94 °C 5 min, followed by 32 cycles of 94 °C for 30 s, 55 °C for 30 s, and 72 °C for 45 s, followed by a single incubation at 72 °C for 5 min. An aliquot of the PCR reaction was removed after cycles 14, 20, 26, and 32. The PCR products were applied to a 1.5% agarose gel and visualized by ethidium bromide staining.

DNA in situ hybridization

Uninfected and HPV 59-infected foreskin xenografts were grown in athymic mice as previously described (Bryan et al., 2000). Early passage ERIN 59 cells (passage 12) and late passage ERIN 59 cells (passage 52) were grown for 14 days in plastic tissue culture flasks in complete F medium containing 2 mM calcium chloride. Medium was removed, and the adherent cell mass was scraped from the flask. Cells were fixed in zinc-formalin and embedded in paraffin. Four micrometer sections were prepared, and one section was stained with hematoxylin and eosin for histologic analysis.

Additional paraffin-embedded sections of cells and foreskin xenografts were fixed by heating for 15 min at 80 °C. Sections were then deparaffinized in xylene followed by ethanol. Sections were treated with 25 μg/mL proteinase K for 5 min at 37 °C followed by 3% H_2O_2 in methanol for 30 min. Sections were washed in PBS, dehydrated by incubation in ethanol, and dried. For detection of HPV 59 DNA sequences, a probe was produced by PCR amplification of the entire 8-kb genome followed by nick translation using biotin-dCTP (Roche Molecular Diagnostics). The HPV 59 DNA probe was added at 5 ng/μL to a DNA in situ hybridization buffer (Dako Corp., Carpenteria, CA). Sections were covered with a HybriSlip (Research Products International, Mount Prospect, IL) and heated at 95 °C for

Table 1
Primer sets, numbers in parentheses indicate position of primers within the HPV 59 genome

GAPDH	5′-GAAGGTGAAGGTCGGAGT-3′; 5′-GAAGATGGTGATGGGATTTC-3′
L1 (6612–6714)	5′-CTACTCGCAGCACCAATCTT-3′; 5′-TCCTCCACATGTCTGGCATA-3′
E1 (1265–1561)	5′-AGCGGCTATGGCTATTCTGA-3′; 5′-CCAATCGCTACAGGTAGTTC-3′
E6/E7 (351–648)	5′-TGAGCTGCTGATACGCTGTT-3′; 5′-GAGTCGGAGTCAGGTAATTG-3′
E2 (3355–3527)	5′-CCAGTGACGAGCAAGTATCC-3′; 5′-TGACACGCTGGTAGACTGAG-3′
E6 (232–367)	5′-ACACCGTATGCAGCGTGTCT-3′; 5′-AGCGTATCAGCAGCTCATGT-3′
E7 (521–865)	5′-AGATCTGTGAAACACTGGTGTAAAACAATG-3′; 5′-GCGGCCGCTTACTGGTTTGCTGCACACAAA-3′
Involucrin	5′-TCCTCCAGTCAATACCCATC-3′; 5′-AGTTGCTCATCTCTCTTGACT-3′

10 min. Probe and target DNA were allowed to hybridize overnight at 37 °C. Sections were washed in 20% formamide in 2× SSC plus 0.05% Tween-20 for 10 min at 37 °C, followed by an additional wash in 2× SSC plus 0.05% Tween-20 for 10 min at 37 °C. Sections were blocked and probes were detected using the Tyramide Signal Amplification Cyanine 3 System as instructed by the manufacturer (PerkinElmer Inc., Shelton, CT). Sections were dehydrated in ethanol and mounted using Vectashield (Vector Laboratories, Burlingame, CA). Slides were viewed using a fluorescent microscope at 590 nm wavelength.

Amplification of papillomavirus oncogene transcript (APOT)

Total RNA was harvested from late passage ERIN 59 cells (passage 72) using RNAaqueous-4PCR (Ambion, Inc.). Total RNA (875 ng) was reverse transcribed with an oligo $(dT)_{17}$-primer coupled to a linker sequence [$(dT)_{17}$-p3, 5′-GACAGACGCTACCACATCACTTTTTTTTTTTTTT-TTT-3′] using the RETROscript Kit One-Step RT-PCR (Ambion) for 20 min at 42 °C in a final volume of 25 μL. To control for RNA and cDNA quality, PCR reactions using GAPDH specific primers were performed as a control. First strand cDNA containing viral oncogene sequences were then amplified by PCR using the primers: HPV 59 E7-specific oligonucleotide p1-59 (5′-CTGACTCCGACTCCGAGAAT-3′) as the forward primer and p3 (5′-GACAGACGCTAC-CACATCAC-3′) as the reverse primer. One microliter of the forward and reverse primer pair (10 μM/primer final concentration) was added to the reaction following the reverse transcription step. The reaction then underwent an initial denaturation step of 94 °C for 2 min, followed by 30 cycles of denaturation at 94 °C for 30 s, annealing at 55 °C for 30 s, elongation at 72 °C for two min, and a final elongation step at 72 °C for 5 min. Five microliters of the amplification product was used as a template for nested PCR with forward primer p2-59+ATT (5′-CTGAACCA-CAGCGTCACAACATT-3′) and $(dT)_{17}$-p3 as reverse primer using SuperTaq (Ambion) in a 50-μL reaction and the same cycling parameters described above. The final PCR products were separated by electrophoresis on 1% agarose gels and visualized by ethidium bromide staining. Visible bands were individually cut from the gel, then eluted using GeneClean Turbo (Qbiogene, Carlsbad, CA). The purified amplimers were cloned using pCRII-TOPO TA cloning kit (Invitrogen) and subjected to single pass primer extension sequence analysis (ACGT, Inc.).

The sequenced transcript was independently verified by RT-PCR using total RNA from late passage ERIN 59 cells (passage 85), using the RETROscript Kit One-Step RT-PCR (Ambion) with the following primers: a forward primer at HPV 59 nt 50 (just upstream from the start of the E6 ORF: 5′-ACGGCATGGCACGCTTTGA-3′, and a reverse primer at nt 2753 within the E2 ORF: 5′-GTCCATCACTGTCTG-CATCTTC-3′). The following cycling parameters were used: reverse transcription at 42 °C for 20 min, 94 °C for two min, then 32 cycles of 94 °C for 30 s, 55 °C for 30 s, and 72 °C for 45 s. The resulting amplimer was gel purified and subjected to single pass primer extension analysis (ACGT, Inc.).

Limiting cycle RT-PCR—viral transcripts

Total RNA was harvested from early passage ERIN 59 cells (passage 9) and late passage ERIN 59 cells (passage 73) using RNAaqueous-4PCR (Ambion). RT-PCR was performed using 500 ng total RNA with the RETROscript Kit One-Step RT-PCR (Ambion). Primers used are described in Table 1 with the following cycling parameters: reverse transcription at 42 °C for 20 min, 94 °C for 2 min, then 32 cycles of 94 °C for 30 s, 55 °C for 30 s, and 72 °C for 45 s. Aliquots of RT-PCR products were removed after cycles 14, 20, 26, and 32 and applied to a 1.5% agarose gel, then visualized with ethidium bromide staining.

Limiting cycle RT-PCR—markers of differentiation

PHKs, early passage ERIN 59 cells (passage 12), and late passage ERIN 59 cells (passage 100) were grown to confluence in complete F medium containing 2 mM calcium chloride as described above. Total RNA was harvested 7 days following addition of calcium chloride, using RNAaqueous-4PCR (Ambion). RNA concentration was determined by spectrophotometry, and RT-PCR was performed on equivalent quantities of total RNA using the RETROscript Kit One-Step RT-PCR (Ambion). Primers used are described in Table 1 with the following cycling parameters: reverse transcription at 42 °C for 20 min, 94 °C for 2 min, then 32 cycles of 94 °C for 30 s, 55 °C for 30 s, and 72 °C for 45 s, followed by a single incubation at 72 °C for 5 min. Aliquots of RT-PCR products were removed after cycles 14, 20, 26, and 32. The RT-PCR products were applied to a 1.5% agarose gel and visualized with ethidium bromide staining. Densitometry readings of GAPDH amplimers from each sample at cycles 14, 20, 26, and 32 were performed to verify that RNA samples were balanced.

Morphological analysis of cells induced to differentiate

PHKs, early passage ERIN 59 cells (passage 12), and late passage ERIN 59 cells (passage 52) were grown as described above. After reaching confluence, 2 mM calcium chloride was added to culture medium, and cells were grown for an additional 14 days. Medium was removed, and the adherent cell mass was scraped from the flask. Cells were fixed in zinc-formalin, and paraffin-embedded tissue sections were prepared. Four-micrometer sections were prepared, and one section was stained with hematoxylin and eosin for histologic analysis.

Immunohistochemistry to detect differentiation-related proteins

To detect involucrin (a cornified cell envelope protein) and the HPV 59 L1 major capsid protein, PHKs, early passage ERIN 59 cells (passage 12) and late passage ERIN 59 cells (passage 52) were grown and induced to differentiate as described above. Cells were harvested and paraffin-embedded sections were prepared as described above. Sections were deparaffinized with xylene and ethanol, treated with 3% H_2O_2 in methanol to reduce endogenous peroxidase activity, and blocked with non-specific rabbit serum. Sections were incubated in either a mouse monoclonal antibody against involucrin (Novocastra, Newcastle upon Tyne, United Kingdom) at 1:100 dilution, or to detect the L1 major capsid protein, an anti-L1 serum (from rabbits immunized with a bacterially expressed HPV 11 trpE-L1 fusion protein) at 1:500 dilution. Preimmune rabbit serum was used as a control. Antibody binding was detected using the Vectastain ABC detection system (Vector Laboratories) to yield a purple precipitate. Slides were examined by light microscopy.

Acknowledgments

This study was funded by NIH (NIAID) AI51524 (Dr. Brown) and AI49254 (Dr. Roman).

References

Aaronson S.A., 1991. Growth factors and cancer. Science, 254, 1146–1153.

Alazawi W., Pett M., Arch B., Scott L., Freeman T., Stanley M.A., Coleman N., 2002. Changes in cervical keratinocyte gene expression associated with integration of human papillomavirus 16[1]. Cancer Res., 62, 6959–6965.

Auvinen E., Hietanen S., Gissmann L., Alonso A., 1998. Human papillomavirus type 33 DNA and E6–E7 transcripts in late passages of the UT-DEC-1 vaginal keratinocyte cell line. Mol. Cell. Probes, 12 (1), 59–62.

Badaracco G., Venuit A., Sedati A., Marcante M.L., 2002. HPV16 and HPV18 in genital tumors: significantly different levels of viral integration and correlation to tumor invasiveness. J. Med. Virol., 67, 574–582.

Barzon L., Pizzighella S., Corti L., Mengoli C., Palu G., 2002. Vaginal dysplastic lesions in women with hysterectomy and receiving radiotherapy are linked to high-risk human papillomavirus. J. Med. Virol., 67, 401–405.

Bechtold V., Beard P., Raj K., 2003. Human papillomavirus type 16 E2 protein has no effect on transcription from episomal viral DNA. J. Virol., 77 (3) 2021–2028.

Bernard B.A., Bailly C., Lenoir M.-C., Darmon M., Thierry F., Yaniv M., 1989. The human papillomavirus type 18 (HPV 18) E2 gene product is a repressor of the HPV 18 regulatory region in human keratinocytes. J. Virol., 63, 4317–4324.

Bezerra A.L., Lopes A., Landman G., Alencar G.N., Torloni H., Villa L.L., 2001. Clinicopathologic features and human papillomavirus DNA prevalence of warty and squamous cell carcinoma of the penis. Am. J. Surg. Pathol., 25, 673–678.

Bryan J.T., Tekchandani J., Schroeder J.M., Brown D.R., 2000. Propagation of human papillomavirus type 59 in the athymic mouse xenograft system. Intervirology, 43 (2), 112–118.

Cooper K., Herrington C.S., Stickland J.E., Evans M.F., McGee J.O.D., 1991. Episomal and integrated human papillomavirus in cervical neoplasia shown by non-isotopic in situ hybridisation. J. Clin. Pathol., 44 (12), 990–996.

Daling J.R., Madeleine M.M., Schwartz S.M., Shera K.A., Carter J.J., McKnight B., Porter P.L., Galloway D.A., McDougall J.K., Tamimi H., 2002. A population-based study of squamous cell vaginal cancer: HPV and cofactors. Gynecol. Oncol., 84, 263–270.

Das B.C., Sharma J.K., Gopalakrishna V., Luthra U.K., 1992. Analysis by polymerase chain reaction of the physical state of human papillomavirus type 16 DNA in cervical preneoplastic and neoplastic lesions. J. Gen. Virol., 73, 2327–2336.

De Geest K., Turyk M.E., Hosken M.I., Hudson J.B., Laimins L.A., Wilbanks G.D., 1993. Growth and differentiation of human papillomavirus type 31b positive human cervical cancer cell lines. Gynecol. Oncol., 49, 303–310.

Demeret C., Desaintes C., Yaniv M., Thierry F., 1997. Different mechanisms contribute to the E2-mediated transcriptional repression of human papillomavirus type 18 viral oncogenes. J. Virol., 71 (12), 9343–9349.

Dillner J., von Krogh G., Horenblas S., Meijer C., 2000. Etiology of squamous cell carcinoma of the penis. Scand. J. Urol. Nephrol., Suppl., 205, 189–193.

Dowhanick J.J., McBride A.A., Howley P.M., 1995. Suppression of cellular proliferation by the papillomavirus E2 protein. J. Virol., 69 (12), 7791–7799.

El Awady M.K., Kaplan J.B., O'Brien S.J., Burk R.D., 1987. Molecular analysis of integrated human papillomavirus 16 sequences in the cervical cancer cell line SiHa. Virology, 159, 389–398.

Evans M.F., Cooper K., 2004. Human papillomavirus integration: detection by in situ hybridization and potential clinical application. J. Pathol., 202, 1–4.

Evans M.F., Mount S.L., Beatty B.G., Cooper K., 2002. Biotinyl-tyramide-based in situ hybridization signal patterns distinguish human papillomavirus type and grade of cervical intraepithelial neoplasia. Mod. Path., 15, 1339–1347.

Fichorova R.N., Rheinwald J.G., Anderson D.J., 1997. Generation of papillomavirus-immortalized cell lines from normal human ectocervical, endocervical, and vaginal epithelium that maintain expression of tissue-specific differentiation proteins. Biol. Reprod., 57 (4), 847–855.

Flores E.R., Lambert P.F., 1997. Evidence for a switch in the mode of human papillomavirus type 16 DNA replication during the viral life cycle. J. Virol., 71 (10), 7167–7179.

Flores E.R., AllenHoffmann B.L., Lee D., Sattler C.A., Lambert P.F., 1999. Establishment of the human papillomavirus type 16 (HPV-16) life cycle in an immortalized human foreskin keratinocyte cell line. Virology, 262 (2), 344–354.

Gillitzer E., Chen G., Stenlund A., 2000. Separate domains in E1 and E2 proteins serve architectural and productive roles for cooperative DNA binding. EMBO J., 19 (12), 3069–3079.

Gross G., Pfister H., 2004. Role of human papillomavirus in penile cancer, penile intraepithelial squamous cell neoplasias and in genital warts. Med. Microbiol. Immunol., 193, 35–44.

Herlyn M., Kath R., Williams N., Valyi-Nagy I., Rodeck U., 1990. Growth-regulatory factors for normal, premalignant, and malignant human cells in vitro. Adv. Cancer Res., 54, 213–234.

Hernadi Z., Sapy T., Krasznai Z.T., 2004. The prevalence of the HPV 16 genome, integrated viral status and p53 genotype in cervical cancer population of north-eastern Hungary, the correlation with the established markers of tumour progression. Eur. J. Obstet. Gynecol. Reprod. Biol., 113, 83–86.

Hietanen S., Auvinen E., Grenman S., Lakkala T., Sajantila A., Klemi P., Maenpaa J., 1992. Isolation of 2 keratinocyte cell lines derived

from HPV-positive dysplastic vaginal lesions. Int. J. Cancer, 52 (3), 391–398.
Hopman A.H., Smedts F., Dignef W., Ummelen M., Sonke G., Mravunac M., Vooijs G.P., Speel E.J., Ramaekers F.C., 2004. Transition of high-grade cervical intraepithelial neoplasia to micro-invasive carcinoma is characterized by integration of HPV 16/18 and numerical chromosome abnormalities. J. Pathol., 202, 23–33.
Hudelist G., Manavi M., Pischinger K.I., Watkins-Riedel T., Singer C.F., Kubista E., Czerwenka K.F., 2004. Physical state and expression of HPV DNA in benign and dysplastic cervical tissue: different levels of viral integration are correlated with lesion grade. Gynecol. Oncol., 92, 873–880.
Hummel M., Hudson J.B., Laimins L.A., 1992. Differentiation-induced and constitutive transcription of human papillomavirus type 31b in cell lines containing viral episomes. J. Virol., 66, 6070–6080.
Jeon S., Lambert P.F., 1995. Integration of human papillomavirus type 16 DNA into the human genome leads to increased stability of E6 and E7 mRNAs: implications for cervical carcinogenesis. Proc. Natl. Acad. Sci. U.S.A., 92 (5), 1654–1658.
Jeon S., Allen-Hoffmann B.L., Lambert P.F., 1995. Integration of human papillomavirus type 16 into the human genome correlates with a selective growth advantage of cells. J. Virol., 69 (5), 2989–2997.
Kerstens H.M., Poddighe P.J., Hanselarr A.G., 1995. A novel in situ hybridization signal amplification method based on the deposition of biotinylated tyramine. J. Histochem. Cytochem., 43, 347–352.
Klaes R., Woerner S.M., Ridder R., Wentzensen N., Duerst M., Schneider A., Lotz B., Melsheimer P., Doeberitz M.V., 1999. Detection of high-risk cervical intraepithelial neoplasia and cervical cancer by amplification of transcripts derived from integrated papillomavirus oncogenes. Cancer Res., 59 (24), 6132–6136.
Koutsky L., 1997. Epidemiology of genital human papillomavirus infection. Am. J. Med., 102 (5A), 3–8.
Lazo P.A., 1987. Structure, DNaseI hypersensitivity and expression of integrated papilloma virus in the genome of HeLa cells. Eur. J. Biochem., 165, 393–401.
Lehr E.E., Qadadri B., Brown C., Brown D.R., 2003. Human papillomavirus type 59 immortalized keratinocytes express late viral proteins and infectious virus after calcium stimulation. Virology, 314, 562–571.
Lizard G., Roignot P., BrunetLecomte P., Chardonnet Y., 1998. Morphological analysis of in situ hybridization signals in cervical intraepithelial neoplasia containing human papillomavirus type 16 or 18: relationship with histological grade and DNA content. Cytometry, 34 (4), 180–186.
Logani S., Lu D., Quint W.G., Ellenson L.H., Pirog E.C., 2003. Low-grade vulvar and vaginal intraepithelial neoplasia: correlation of histologic features with human papillomavirus DNA detection and MIB-1 immunostaining. Mod. Path., 16, 735–741.
McBride A.A., Howley P.M., 1991. Bovine papillomavirus with a mutation in the E2 serine 301 phosphorylation site replicates at a high copy number. J. Virol., 65, 6528–6534.
Nishimura A., Ono T., Ishimoto A., Dowhanick J.J., Frizzell M.A., Howley P.M., Sakai H., 2000. Mechanisms of human papillomavirus E2-mediated repression of viral oncogene expression and cervical cancer cell growth inhibition. J. Virol., 74 (8), 3752–3760.
Ozbun M., 2002. Human papillomavirus type 31b infection of human keratinocytes and the onset of early transcription. J. Virol., 76 (22), 11291–11300.
Ozbun M.A., Meyers C., 1997. Characterization of late gene transcripts expressed during vegetative replication of human papillomavirus type 31b. J. Virol., 71 (7), 5161–5172.
Peitsaro P., Hietanen S., Johansson B., Lakkala T., Syrjanen S., 2002. Single copy heterozygote integration of HPV 33 in chromosomal band 5p14 is found in an epithelial cell clone with selective growth advantage. Carcinogenesis, 23, 1057–1064.
Pett M.R., Alazawi W.O., Roberts I., Dowen S., Smith D.I., Stanley M.A., Coleman N., 2004. Acquisition of high-level chromosomal instability is associated with integration of human papillomavirus type 16 in cervical keratinocytes. Cancer Res., 64, 1359–1368.
Rho J., Roy-Burman A., Kim H., de Villiers E.M., Matsukura T., Choe J., 1994. Nucleotide sequence and phylogenetic classification of human papillomavirus type 59. Virology, 203 (1), 158–161.
Rho J., deVilliers E.M., Choe J., 1996. Transforming activities of human papillomavirus type 59 E5, E6 and E7 open reading frames in mouse C127 cells. Virus Res., 44 (1), 57–65.
Robboy S.J., Anderson M.C., Russell P., 2002. Pathology of the Female Reproductive Tract. Churchill Livingstone, London.
Romanczuk H., Howley P.M., 1992. Disruption of either the E1 or E2 regulatory gene of human papillomavirus type 16 increases viral immortalization capacity. Proc. Natl. Acad. Sci. U.S.A., 89, 3159–3163.
Sano T., Hikino T., Niwa Y., Kashiwabara K., Oyama T., Fukuda T., Nakajima T., 1998. In situ hybridization with biotinylated tyramide amplification: detection of human papillomavirus DNA in cervical neoplastic lesions. Mod. Path., 11 (1), 19–23.
Schiffman M.H., Brinton L.A., 1995. The epidemiology of cervical carcinogenesis. Cancer, 76 (Suppl. 10), 1888–1901.
Schiffman M.H., Burk R.D., 1997. Human papillomaviruses. In: Evans, A.S., Kaslow, R.A. (Eds.), Viral Infections of Humans. Plenum Medical Book Company, New York, pp. 983–1022.
Stanley M.A., Browne H.M., Apeleby M., Minson A.C., 1989. Properties of a non-tumorigenic human cervical keratinocyte cell line. Int. J. Cancer, 43, 672–676.
Sterling J., Stanley M., Gatward G., Minson T., 1990. Production of human papillomavirus type 16 virions in a keratinocyte cell line. J. Virol., 64, 6305–6307.
Sterling J.C., Skepper J.N., Stanley M.A., 1993. Immunoelectron microscopical localization of human papillomavirus type 16 L1 proteins and E4 proteins in cervical keratinocytes cultured in vivo. J. Invest. Dermatol., 100 (2), 154–158.
Stupar M., 1989. The presence of human papillomavirus-16 genome in the CaSki cervical carcinoma DNA. Iugosl. Physiol. Pharmacol. Acta, 25, 45–52.
Thierry F., Howley P.M., 1991. Functional analysis of E2-mediated repression of the HPV 18 P105 promoter. New Biol., 3, 90–100.
van Beurden M., ten Kate F.W., Tjong-A-Hung S.P., de Craen A.J., van der Vange N., Lammes F.B., ter Schegget J., 1998. Human papillomavirus DNA in multicentric vulvar intraepithelial neoplasia. Int. J. Gynecol. Pathol., 17, 12–16.
zur Hausen H., 1991. Human papillomaviruses in the pathogenesis of anogenital cancer. Virology, 184, 9–13.